Technical Notes

TECHNICAL NOTES are short manuscripts describing new developments or important results of a preliminary nature. These Notes should not exceed 2500 words (where a figure or table counts as 200 words). Following informal review by the Editors, they may be published within a few months of the date of receipt. Style requirements are the same as for regular contributions (see inside back cover).

Krypton Performance Optimization in High-Voltage Hall Thrusters

Jesse A. Linnell* and Alec. D. Gallimore[†]
University of Michigan, Ann Arbor, Michigan 48109

Nomenclature

A_{ch} = discharge channel cross-sectional area
b = channel width
e = electron charge
I_B = beam current
K = undefined constant
K' = undefined constant
L_{ch} = channel length
M_i = propellant atom mass
$\dot{m}_a$ = anode mass flow rate
$\dot{m}_i$ = ion mass flow rate
n_e = electron number density
n_i = ion number density
n_n = neutral number density
$Q_{i,n}$ = ionization collision cross section
T_e = electron temperature
T_n = neutral temperature
t_i = characteristic ionization time
t_{res} = neutral residence time
V_D = discharge voltage
V_e = electron velocity
V_i = ion velocity
V_n = neutral particle velocity
$\dot{v}_a$ = anode volumetric flow rate
Z_i = charge state of ith ion species
α = scaling constant using anode mass flow rate
α_V = scaling constant for efficient ionization
η_p = propellant utilization efficiency
Ω_i = current fraction of ith ion species

I. Introduction

HALL thrusters[1,2] are space-propulsion devices that use crossed electric and magnetic fields to ionize and accelerate ions to high exhaust velocities. The electric field is established by an electron current that crosses and is concurrently impeded by an applied magnetic field. Generally, noble gases of high atomic weight are used as propellant, with xenon being the most common choice. However, because of its superior specific impulse and lower cost than xenon, krypton has recently sparked renewed interest in the electric propulsion community as a propellant for Hall thrusters.

Krypton's higher specific impulse could extend Hall-thruster usage to a larger range of mission applications. For example, recent photovoltaic improvements have decreased the power supply mass, which results in an increase in optimal specific impulse for lunar missions above that achievable with conventional xenon Hall thrusters. Although previous studies[3–8] report Hall thrusters using krypton to have a lower thrust efficiency as compared to xenon, results using the NASA-457M[9,10] indicate that it is possible to operate krypton at efficiencies comparable to those achieved with xenon. Xenon and krypton performance measurements and Faraday probe measurements taken on the NASA-173Mv1 are presented next. From these results, it is possible to find approximate anode flow rates and discharge voltages for optimum efficiency with krypton. Scaling relations are also used to define methods for improving krypton efficiency.

II. Efficiency Optimization Scaling

Several researchers have suggested that the reason for the efficiency gap between xenon and krypton is largely a result of propellant utilization efficiency.[4,5,8] This theory is confirmed in Sec. IV after a simple scaling for ionization optimization is presented. Although the focus of this analysis is krypton ionization optimization, a similar analysis is applicable for xenon operation conditions where propellant utilization is low (e.g., low discharge voltages). Beam divergence has also been found to be a significant contributor to the xenon-krypton efficiency gap[11]; however, this analysis is out of the scope of this paper.

For efficient ionization, the neutral residence time should be longer than the time required for electron impact ionization. The time rate of change from neutrals to ions is equal to the total collision rate ($dn_n/dt = -n_e n_n \langle Q_{i,n} V_e \rangle$). Therefore, the characteristic ionization time is given by $t_i = 1/(n_e \langle Q_{i,n} V_e \rangle)$, which must be less than the neutral residence time. By approximating the residence time as the channel length divided by the neutral particle velocity, a relation for the ratio of times is given in Eq. (1):

$$t_{res}/t_i = L_{ch} n_e \langle Q_{i,n} V_e \rangle / V_n \qquad (1)$$

By assuming quasineutrality ($n_i \approx n_e$) to relate the electron number density to the ion flux and assuming that the ion flux is proportional to and approximately equal to the total heavy particle flux through the anode, we can simplify the electron number density [$n_e \approx n_i \approx K' \dot{v}_a/(A_{ch} V_i)$]. Propellant utilization is approximately 90% for xenon and 80–85% for krypton.[11] To first-order accuracy, K' can be considered approximately equal for both propellants. In reality, because of the propellant utilization difference, the value of K' is approximately 10% higher for xenon as compared to krypton.

By inserting standard relations for the neutral and electron velocities, relating ion velocity to the discharge voltage, and by noting that in the electron energy range of interest the ionization collision cross section is approximately constant,[12] one can arrive at a simple expression for Hall-thruster optimization [Eq. (2)]:

$$t_{res}/t_i = K[M_i Q_{i,n}]\dot{v}_a(L_{ch}/A_{ch})\sqrt{T_e/T_n V_D} \qquad (2)$$

When Eq. (2) is maximized, ionization efficiency is optimized. For the same reasons as K', K is about 10% higher for xenon as compared to krypton, but can be considered approximately equal for both propellants. Anode volumetric flow rate is used because it is a measure of the total propellant atoms injected into the discharge channel and because of this, it is a more fundamental quantity for understanding ionization processes.

Equation (2), which is effectively the same scaling relations found by Kim et al.,[4] suggests that propellant utilization will be improved for increased anode flow rate, channel length, and electron temperature. The propellant utilization will also improve when neutral temperature and channel area for a given anode flow rate are reduced. Discharge dimensions can indeed be exploited to optimize krypton efficiency, but for the current discussion the discharge channel dimensions are fixed. It is also possible that the neutral temperature can be managed by active or passive thermal control of the anode and discharge channel walls. Although this suggests a new important design consideration, this experimental setup is incapable of Hall thruster thermal control. The most obvious factor that improves propellant utilization is anode flow rate, which is the focus of the later discussion.

As the discharge voltage increases, it would appear that ionization efficiency would decrease, but in fact the opposite is true. Ionization efficiency improves at high voltages because of changes in the electron temperature and thus the ionization collision cross section. At low discharge voltages, electron temperatures increase linearly (because of Joule heating) with discharge voltage.[13−15] Moreover, the ionization collision cross section for krypton also increases nearly linearly below an electron temperature of approximately 40 eV (Ref. 12). However, with discharge voltages between approximately 400–700 V, the electron temperature saturates[13−15] near 50–60 eV, which results in a plateau in ionization efficiency.

The behavior of the bracketed constant in Eq. (2) is worth exploring. Figure 1 shows that above an electron temperature of about 30 eV [approximate discharge voltage of 300 V (Ref. 16)] the ratio of krypton-to-xenon total electron impact ionization collision cross section is almost constant at 0.68. If the Hall thruster is operating above a discharge voltage of 300 V with xenon and krypton, the bracketed coefficient given in Eq. (2) will be 2.3 times lower for krypton, which shows the difficulty in operating krypton efficiently. At electron temperatures below 30 eV (discharge voltages below ∼300 V), it is probably nearly impossible for krypton to rival xenon in performance.

It should be possible to determine a scaling constant that indicates the point at which efficient ionization is reached. Equation (3) gives this constant as a function of discharge channel dimensions and anode flow rate. This constant should be consistent for a large range of thruster sizes assuming that different thrusters are operating at similar conditions (e.g., matched discharge voltage, electron temperature, and thruster thermal temperature). Each propellant will have its own unique value of α_V. Krypton's value of α_V is expected

to be approximately twice as high as xenon's α_V value.

$$\alpha_V = \dot{v}_a(L_{\text{ch}}/A_{\text{ch}}) \tag{3}$$

Equation (3) is analogous to the relation found by Morozov and Melikov[17] and Bugrova et al.,[18] which is shown in Eq. (4). In Eq. (4), volumetric flow rate is replaced with mass flow rate, and channel length is replaced by the channel width. Channel width is chosen for their scaling constant because they say that channel width is characteristic of the region with significant electric fields. According to Kim,[19] discharge channel length and width scale proportionally, so that either choice for scaling is probably equivalent. Bugrova et al.[18] suggest that the value of α is approximately constant at 0.02 mg/(s mm) and is similar for both krypton and xenon.[7] For reasons discussed earlier, krypton's α value is expected to be as much as 50% higher than xenon's α value. The use of mass flow rate instead of volumetric flow rate reduces the difference in the α value for krypton and xenon caused by the difference in atomic mass. There is not enough information about the electron energy distribution to give a conclusive statement as to the difference in the value of α between krypton and xenon. To be consistent with previous work, the value of α derived by Bugrova et al. will be used in the following analysis.

$$\alpha = \dot{m}_a(b/A_{\text{ch}}) \tag{4}$$

III. Experimental Apparatus and Techniques

A. Facility

The measurements reported in this paper were conducted in the Large Vacuum Test Facility (LVTF) at the University of Michigan's Plasmadynamics and Electric Propulsion Laboratory. The LVTF is a cylindrical stainless-steel tank that is 9 m long and 6 m in diameter. The vacuum chamber is evacuated using 7 CryoVac Inc. model TM-1200 internal cryopumps. The pumps are capable of pumping 240,000 l/s of xenon and 252,000 l/s of krypton. The pressure is monitored with two hot-cathode ionization gauges. The vacuum chamber operates at a base pressure of 2.0×10^{-7} torr with an operation pressure of approximately 3.2×10^{-6} torr (corrected[20]) for most of thruster operation points.

Research-grade xenon and krypton are used as propellants for all reported measurements. The purity level of xenon and krypton are 99.9995 and 99.999%, respectively. The propellants are supplied through propellant feed lines using 20- and 200-sccm mass flow controllers for the cathode and anode, respectively. For the high discharge current krypton points a 500-sccm mass flow controller is used. The mass flow controllers are calibrated using a constant-volume method, and the compressibility correction factor is calculated using the van der Waals equation[21] and the virial equation.[22] The mass flow calibration is monitored every few seconds and converges when the 5-sigma confidence interval around the average calculated flow rate decreases to below the manufacturer's error specification (±1% of full scale).

B. Thruster

The NASA-173Mv1 Hall effect thruster[23] is used to characterize the performance of krypton propellant. In addition to the standard inner and outer magnetic coils, the NASA-173Mv1 uses a trim coil to shape the magnetic field topology. The added magnetic field control offered by the trim coil is found to improve thruster efficiency by providing both a magnetic plasma lens through the bulk of the channel width and magnetic mirrors at the channel wall. Both features tend to focus the electrons and ions toward the center of the discharge channel. The plasma lens has been shown to improve thruster efficiency by improving beam focusing, ion acceleration processes, and the electron dynamics.[11,16,23]

A Busek BHC-50-3UM cathode is used for this experiment. For most of the thruster operation points, the cathode flow rate is equal to 10% of the anode flow rate. Although, the cathode requires a minimum flow rate of 0.93 sccm to operate on design. The cathode axial centerline is mounted at a 30-deg angle with respect to the
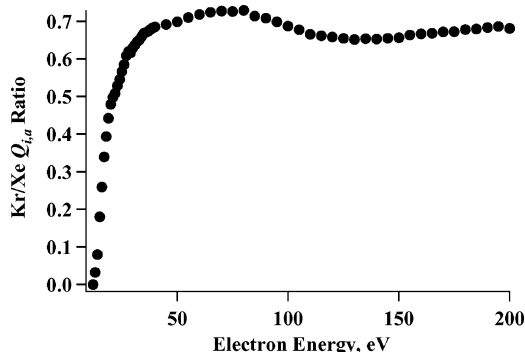

Fig. 1   Ratio of krypton to xenon total electron-atom impact ionization collision cross section vs electron energy.

thruster axial direction, and the center of the cathode orifice is placed 30 mm downstream and 30 mm above the thruster face.

C.   Thrust Stand

The thrust measurements for this experiment are recorded using a NASA Glenn Research Center null-type inverted pendulum thrust stand, the same thrust stand design used with the NASA-457M.[9,10] Error in thrust measurements is approximately ±1% of full scale.[24] Thruster operation is monitored in real time by an Agilent Datalogger. The monitored properties include the magnet currents and voltages, discharge current, and thrust. The mass flow rate and discharge voltage are kept constant during the thruster tuning and for this reason are monitored manually. Currents are measured by monitoring calibrated shunts, and the discharge current is monitored via a current probe. The shunts and current probe are calibrated before the experiment using a digital multimeter. The error associated with the multimeter is ±0.4% for dc voltage measurements and ±1.5% for dc current measurements. The current probe has approximately ±1.5% error.

The real-time efficiency is calculated from the monitored Hall-thruster conditions. The magnets are then varied to find the true peak efficiency. The Hall thruster is optimized over a period of 30 min to two hours to reach a steady operation point.

Thrust, anode specific impulse, and anode efficiency measurement uncertainties are found by accounting for all aforementioned errors. Thrust measurements have ±4.13 mN error, anode specific impulse measurements have approximately ±2.5% error, and efficiency measurements have on average ±5% error.

D.   Magnetically Filtered Faraday Probe

Faraday probe data are collected using the magnetically filtered Faraday probe (MFFP).[24,25] Facility effects and high backpressures can result in the overprediction of ion current, caused by the collection of charge-exchange (CEX) ions. The MFFP has been shown to be very effective at excluding CEX ions. The MFFP has a collector surrounded by a box with a magnetic field applied inside the box resulting in a dual-mode ion filtration system. The magnetic field alters the trajectory of ions such that ions with kinetic energies below 20 eV are deflected away from the collector. In addition, the box surrounding the collector acts as a geometric collimator that further reduces CEX ion collection. The reported results are corrected to take into account the collimation provided by the box.[26] The MFFP collector is spray coated with tungsten in order to reduce secondary electron emission.[27,28] Beam attenuation caused by CEX and elastic collisions are also accounted for by using the correction factor developed Sovey and Patterson.[29]

The MFFP is mounted on a radial arm 1 m downstream of the thruster exit plane. The beam current is calculated from the Faraday probe data by integrating from 0 to 90 deg in spherical cordinates.[30] It is then possible to calculate propellant utilization efficiency by using Eq. (5) (Refs. 23 and 31). Species fraction results from Ref. 11 are incorporated to calculate propellant utilization.

$$\eta_p = \frac{\dot{m}_i}{\dot{m}_a} = \frac{M_i I_B}{(\dot{m}_a e)} \sum \frac{\Omega_i}{Z_i} \qquad (5)$$

IV.   Discussion and Experimental Results

A.   Specific-Impulse Comparison

Although an efficiency gap does exist between xenon and krypton, Fig. 2 shows the superior anode specific impulse of krypton. If the efficiency gap can be understood and minimized, krypton will become a legitimate option for Hall-thruster operation. The points presented in Fig. 2 operate at discharge voltages ranging from 300 to 800 V and discharge currents ranging from 5–16 A.

B.   Voltage Trends

Anode efficiency vs discharge voltage at constant flow rate is shown in Fig. 3. There are three curves in this figure: one xenon curve, a krypton curve matching xenon volumetric flow rate, and a krypton curve matching xenon power. Krypton efficiency improves,
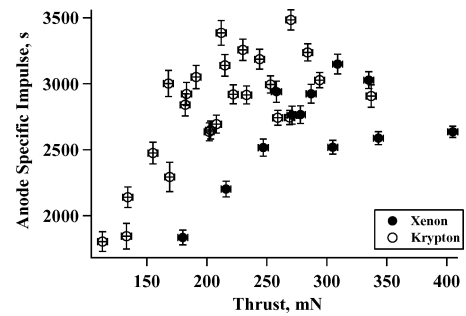
Fig. 2   Krypton and xenon anode specific impulse vs thrust.
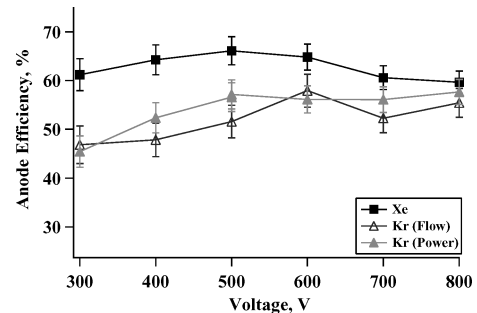
Fig. 3   Anode efficiency vs discharge voltage at 102.4-sccm anode flow rate.

and the efficiency gap between xenon and krypton narrows with increasing discharge voltage. At low voltage, the absolute anode efficiency gap is approximately 15%, and as voltage is increased the efficiency gap is reduced to 2%. Also, the krypton efficiency improves with increased anode flow rate. The power matched flow rate curve has higher anode efficiency than the flow rate matched curve and has approximately 25% higher anode flow rate. The 500-V peak in the xenon curve might be because of a number of different efficiency components. Although the krypton power matched line shows a similar peak at 500 V, this trend is much less clear in the krypton lines because of the dominant role that propellant utilization plays.

The flow rate and voltage trends shown in Fig. 3 indicate that propellant utilization is likely responsible for the efficiency gap. Increasing krypton anode flow rate increases the neutral number density and the ionizing collision frequency. As discharge voltage increases, the electron temperature increases and plateaus at around 50–60 eV (Refs. 13–15). Because the main contributor to the electron temperature saturation is losses to the wall in a space-charge-limited sheath,[13-15] it is reasonable to assume that the electron temperature will be similar for both xenon and krypton. In fact, internal emissive probe measurements show the maximum electron temperature to be between 50–60 eV for both xenon and krypton.[32] This figure suggests that krypton efficiency plateaus in the electron saturation regime (approximately 400–700 V) and krypton efficiency are optimized above discharge voltages of 500 V.

C.   Flow Rate Trends

To improve the krypton efficiency further, it is important to focus on efficiency trends at different anode flow rates. Figure 4 shows anode efficiency vs anode flow rate for krypton at 500, 600, and 700 V. These voltages are in the electron saturation regime discussed earlier and also fall above the suggested voltage minimum for optimized krypton efficiency. At low flow rates, krypton efficiency greatly improves with anode flow rate. However, the anode efficiency plateaus between 55 and 60% as anode flow rate continue to increase. Two linear fits are applied to the low-anode flow-rate and high-anode flow-rate sections. The intersection of these lines is located at 114 sccm and defines the point at which the anode efficiency plateau begins. This suggests that in the electron saturation regime optimum krypton efficiency is reached when α is equal to

Table 1   Operation points of interest for the Faraday probe analysis

Point no.	Propel.	V_D, V	I_D, A	Discharge power, W	Anode flow, mg/s (sccm)	Cathode flow, mg/s	Inner coil, A	Outer coil, A	Trim coil, A	Thrust, mN	I_{SP}, s	Anode effic., %	Propel. util., %
1	Xe	700	8.57	5999	8.94 (91.59)	0.90	2.81	2.95	−1.48	258	2940	62.0	86.5
2	Kr	700	11.42	7994	**8.94** (143.52)	0.89	2.20	2.52	−0.51	284	3237	56.4	78.7
3	Kr	700	**8.57**	**5999**	6.98 (112.03)	0.70	2.32	2.94	−0.51	215	3140	55.2	78.2
4	Kr	700	7.05	4935	5.70 (**91.56**)	0.57	2.20	2.25	−0.57	168	3002	50.1	75.3
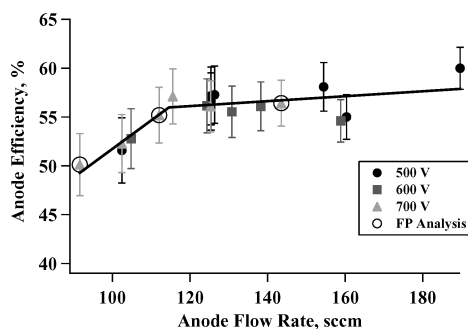
Fig. 4   Krypton anode efficiency vs anode flow rate.
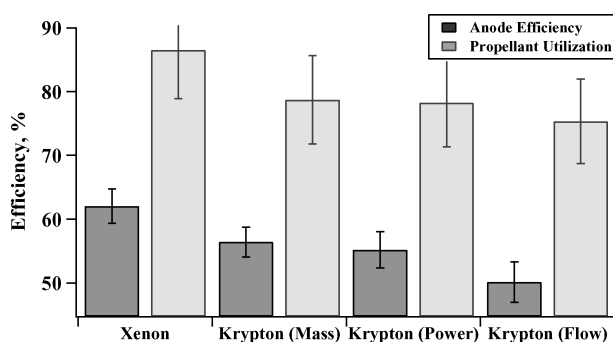
Fig. 5   Anode efficiency and propellant utilization efficiency comparison.

or greater than 0.015 mg/ (mm · s). This criterion should give the necessary neutral number density for efficient krypton operation for a broad range of Hall-thruster sizes.

D.   Performance Analysis

Faraday probe results are presented for the four operation points given in Table 1: xenon operation at 700 V and 6 kW, and three krypton conditions that match the xenon volumetric flow rate, xenon power, and xenon mass flow rate. The krypton points fall above, below, and on the knee of the efficiency optimization curve and are circled in Fig. 4. The relative error associated with calculating propellant utilization from the Faraday probe measurements is estimated as 9% (Ref. 11). Although the propellant utilization magnitude is somewhat imprecise, the relative trends between the data points are expected to be much more accurate.

The anode efficiency and propellant utilization efficiency for these operation points are plotted in Fig. 5. The anode efficiency compared to xenon is relatively 10% lower (absolute difference of about 6–7%) for krypton operating at and above the anode efficiency knee (Fig. 4) and below the efficiency knee the relative difference in anode efficiency is 19%. Above the efficiency knee, the propellant utilization efficiency for krypton has a relative difference of 9% below xenon. Below the efficiency knee the relative propellant utilization efficiency gap increases to 13%. These trends confirm the theory that the efficiency gap for krypton is strongly related to the propellant utilization efficiency.

V.   Conclusions

The results show that krypton has lower anode efficiency than xenon with an absolute efficiency gap between 2 to 15%. However, even with the efficiency gap, krypton has a superior specific impulse to xenon. The efficiency gap between xenon and krypton is shown to be related to krypton's inferior propellant utilization. At sufficient anode flow rates and discharge voltages, the krypton anode efficiency is capable of reaching levels between 55–60%. It is found that krypton efficiency is optimized above a discharge voltage of 500 V and with an α value of at least 0.015 mg/(mm · s). Even as the krypton propellant utilization is optimized, the propellant utilization efficiency is still approximately 9% lower relative to xenon's.

A simple scaling analysis reveals the courses that can be taken to maximize krypton ionization. Propellant utilization efficiency can be improved by increasing anode flow rate, channel length, and electron temperature. Electron temperature is difficult to control as a result of electron temperature saturation, although significant efficiency improvements are gained by increasing the discharge voltage. Increasing electron temperature also has the added benefit of increasing the ionization collision cross section. Propellant utilization can also be improved by reducing discharge channel area for a given anode flow rate and reducing the neutral temperature. To this last point, thruster thermal management to reduce neutral atom temperature has not been a focus of Hall-thruster design, but could potentially be an effective way of improving propellant utilization efficiency.

Acknowledgments

References

[1]Kim, V., "Main Physical Features and Processes Determining the Performance of Stationary Plasma Thrusters," *Journal of Propulsion and Power*, Vol. 14, No. 5, 1998, pp. 736–746.

[2]Zhurin, V. V., Kaufman, H. R., and Robinson, R. S., "Physics of Closed Drift Thrusters," *Plasma Sources Science and Technology*, Vol. 8, No. 1, 1999, pp. R1–R20.

[3]Marrese, C., Haas, J. M., Domonkos, M. T., Gallimore, A. D., Tverdokhlebov, S., and Garner, C. E., "The D-100 Performance and Plume Characterization of Krypton," AIAA Paper 96-2969, July 1996.

[4]Kim, V., Popov, G., Kozlov, V., Skrylnikov, A., and Grdlichko, D., "Investigation of SPT Performance and Particularities of its Operation with Krypton and Xenon Mixtures," *Proceedings of the 27th International Electric Propulsion Conference*, Paper 2001-065, Oct. 2001.

[5]Semenkin, A. V., and Gorshkov, G. O., "Study of Anode Layer Thruster Operation with Gas Mixtures," *Proceedings of the 24th International Electric Propulsion Conference*, Paper 1995-078, Sept. 1995.

[6]Arkhipov, B. A., Koryakin, A. I., Murashko, V. M., Nesterenko, A. N., Khoromsky, I. A., Kim, V., Kozlov, V. I., Popov, G. A., and Skrylnikov, A. I., "The Results of Testing and Effectiveness of Kr-Xe Mixture Application in SPT," *Proceedings of the 27th International Electric Propulsion Conference*, Paper 2001-064, Oct. 2001.

[7]Bugrova, A. I., Lipatov, A. S., Morozov, A. I., and Churbanov, D. V., "On a Similarity Criterion for Plasma Accelerators of the Stationary Plasma Thruster Type," *Technical Physics Letters*, Vol. 28, No. 10, 2002, pp. 821–823.

[8]Bugrova, A. I., Lipatov, A. S., Morozov, A. I., and Solomatina, L. V., "Global Characteristics of an ATON Stationary Plasma Thruster Operating with Krypton and Xenon," *Plasma Physics Reports*, Vol. 28, No. 12, 2002, pp. 1032–1037.

[9]Manzella, D. H., Jankovsky, R., and Hofer, R. R., "Laboratory Model 50 kW Hall Thruster," AIAA Paper 2002-3676, July 2002.

[10]Jacobson, D. T., and Manzella, D. H., "50 KW Class Krypton Hall Thruster Performance," AIAA Paper 2003-4550, July 2003.

[11]Linnell, J. A., and Gallimore, A. D., "Efficiency Analysis of a Hall Thruster Operating with Krypton and Xenon," AIAA Paper 2005-3683, July 2005.

[12]Wetzel, R. C., Baiocchi, F. A., Hayes, T. R., and Freund, R. S., "Absolute Cross Sections for Electron-Impact Ionization of the Rare-Gas Atoms by the Fast-Neutral-Beam Method," *Physical Review A*, Vol. 35, No. 2, 1987, pp. 559–577.

[13]Raitses, Y., Staack, D., Smirnov, A., and Fisch, N. J., "Space Charge Saturated Sheath Regime and Electron Temperature Saturation in Hall Thrusters," *Physics of Plasmas*, Vol. 12, No. 073507, July 2005.

[14]Ahedo, E., and Escobar, D., "Influence of Design and Operation Parameters on Hall Thruster Performances," *Journal of Applied Physics*, Vol. 96, No. 2, 2004, pp. 983–992.

[15]Barral, S., Makowski, K., Peradzyski, Z., Gascon, N., and Dudeck, M., "Wall Material Effects in Stationary Plasma Thrusters. II. Near-Wall and In-Wall Conductivity," *Physics of Plasmas*, Vol. 10, No. 10, 2003, pp. 4137–4152.

[16]Linnell, J. A., and Gallimore, A. D., "Internal Plasma Structure Measurements of a Hall Thruster Using Plasma Lens Focusing," AIAA Paper 2005-4402, July 2005.

[17]Morozov, A. I., and Melikov, I. V., "Similitude in Hall-Current Plasma Accelerators," *Soviet Physics—Technical Physics*, Vol. 19, No. 3, 1974, pp. 340–342.

[18]Bugrova, A. I., Maslennikov, N. A., and Morozov, A. I., "Similarity Laws for the Global Properties of a Hall Accelerator," *Soviet Physics—Technical Physics*, Vol. 36, No. 6, 1991, pp. 612–615.

[19]Kim, V., Kozlov, V., Lazurenko, A., Popov, G., Skrylnikov, A., Clauss, C., and Day, M., "Development and Characterization of Small SPT," AIAA Paper 1998-3335, July 1998.

[20]Dushman, S., *Scientific Foundations of Vacuum Technique*, Vol. 4, Wiley, New York, 1958.

[21]Lide, D. R., *CRC Handbook of Chemistry and Physics*, 73rd ed., CRC Press, Boca Raton, FL, 1992.

[22]Dymond, J. H., and Smith, E. B., *The Virial Coefficients of Pure Gases and Mixtures, a Critical Compilation*, Oxford Univ. Press, New York, 1980.

[23]Hofer, R. R., "Development and Characterization of High-Efficiency, High-Specific Impulse Xenon Hall Thrusters," Ph.D. Dissertation, Dept. of Aerospace Engineering, Univ. of Michigan, Ann Arbor, MI, 2004.

[24]Walker, M. L. R., "Effects of Facility Backpressure on the Performance and Plume of a Hall Thruster," Master's Thesis, Dept. of Aerospace Engineering, Univ. of Michigan, Ann Arbor, MI, 2005.

[25]Rovey, J. L., Walker, M. L. R., Gallimore, A. D., and Peterson, P. Y., "Magnetically-Filtered Faraday Probe for Measuring the Ion Current Density Profile of a Hall Thruster," *Review of Scientific Instruments*, Vol. 77, No. 013503, 2006, Jan. 2006.

[26]Hofer, R. R., Walker, M. L. R., and Gallimore, A. D., "A Comparison of Nude and Collimated Faraday Probes for Use with Hall Thrusters," *Proceedings of the 27th International Electric Propulsion Conference*, Paper 2001-020, Oct. 2001.

[27]Hagstrum, H. D., "Auger Ejection of Electrons from Tungsten by Noble Gas Ions," *Physical Review*, Vol. 96, No. 2, 1954, pp. 325–335.

[28]Brown, S. C., *Basic Data of Plasma Physics*, American Inst. of Physics, New York, 1994.

[29]Sovey, J. S., and Patterson, M. J., "Ion Beam Sputtering in Electric Propulsion Facilities," AIAA Paper 1991-2117, June 1991.

[30]Manzella, D. H., "Hall Thruster Ion Beam Characterization," AIAA Paper 1995-2927, July 1995.

[31]Hofer, R. R., and Gallimore, A. D., "Efficiency Analysis of a High-Specific Impulse Hall Thruster," AIAA Paper 2004-3602, July 2004.

[32]Linnell, J. A., and Gallimore, A. D., "Internal Plasma Structure Measurements of a Hall Thruster Using Xenon and Krypton Propellant," *Proceedings of the 29th International Electric Propulsion Conference*, Oct.–Nov. 2005.